Application of the continuous wavelet transform to the fluctuations and electric field analysis in the H-1 heliac

X. Shi[a] and J. Boman
Faculty of Engineering and Physical Systems, Central Queensland University, Rockhampton QLD 4701, Australia

M. G. Shats
Plasma Research Laboratory, Australian National University, Canberra ACT 0200, Australia

(Presented on 19 June 2000)

We apply the continuous wavelet transform (CWT) and a CWT spectral technique to the analysis of the time-resolved fluctuation-driven particle flux in the H-1 heliac. The results confirm that in some cases the outward radial flux reverses its direction. In addition, time-resolved frequency spectra of fluctuation signals obtained by CWT show that the dominant frequency component as a function of time closely follows changes in the radial electric field. This suggests that the $V_{E\times B}$ drift velocity dominates the poloidal phase velocity of the fluctuations in the laboratory frame, in which case the time-resolved frequency can be used to characterize the radial electric field. © *2001 American Institute of Physics.* [DOI: 10.1063/1.1310583]

I. INTRODUCTION

The wavelet transform has proven to be a useful tool in time-frequency analysis of transient signals in plasma physics.[1–3] In this article, we apply the continuous wavelet transform (CWT) to the fluctuation signals measured in the H-1 heliac. We reformulate the spectral techniques introduced by Powers,[4] by replacing the Fourier transform with the CWT, to study time-resolved fluctuation-driven particle transport. Time evolution of the dominant frequency component of the fluctuations and its correlation with the radial electric field are also studied. The article is organized as follows. In Sec. II, the CWT and the CWT spectral technique are discussed. In Sec. III the main results are presented, which is followed by a summary in Sec. IV.

II. THE CWT AND ITS APPLICATION TO THE STUDY OF FLUCTUATIONS AND PARTICLE TRANSPORT

The time-frequency spectrum of a nonstationary signal can be obtained using the wavelet transform. The wavelet transform uses a family of compressed and stretched wavelets from a mother wavelet to analyze a signal. These wavelets are known as analyzing wavelets. There are analogies and differences between the wavelet transform and the windowed Fourier transform, also known as the short time Fourier transform (STFT).[5,6] Both transforms use a set of analyzing signals, which have finite effective support in the time domain, and the spectra of these analyzing signals have finite effective support in the frequency domain. The major difference between them is that in the STFT, the analyzing signals have the same time width during the analysis of frequency contents of a signal, while in the wavelet transform, the time widths of analyzing wavelets are adapted to the frequency components they are analyzing. For high frequencies the wavelets are very narrow, and for low frequencies the wavelets are much broader. As a result, the wavelet transform is better able than the STFT to ''zoom in'' on very short-lived high frequency phenomena, such as transients in signals, while still being able to have the low frequency components resolved in the time and frequency domains.

In this article, the continuous wavelet transform is employed, which is defined as

$$C(a,b)=\frac{1}{\sqrt{a}}\int_{-\infty}^{\infty} f(t)\,\psi\left(\frac{t-b}{a}\right)dt, \tag{1}$$

where $f(t)$ is the signal being analyzed, $\psi[(t-b)/a]$ is the analyzing wavelet with a and b being the scale factor and position factor respectively, and $C(a,b)$ are the CWT coefficients. The larger the scale factor a, the longer the wavelet in the time domain. Each analyzing wavelet at a particular scale a analyzes a frequency band of the signal centered at a frequency ω. The scale factor a is inversely proportional to the frequency ω. The position factor b indicates the location of the analyzing wavelet on the time axis. A plot of $C(a,b)$ versus a set of a's and b's gives the time-frequency spectrum of a signal. In our work, a complex Morlet wavelet is used as the mother wavelet in the CWT. The CWT coefficients obtained are also complex numbers containing magnitude and phase information of signal frequency components.

Powers[4] has derived the time-averaged fluctuation-driven particle flux as

$$\langle \tilde{n}\tilde{V}_r\rangle=\frac{1}{B}\langle \tilde{n}\tilde{E}_p\rangle=\frac{2}{B}\mathrm{Re}\int_0^{\infty} p_{\tilde{n}\tilde{E}_p}(\omega)\,d\omega, \tag{2}$$

where the pointed brackets denote a time average, $\tilde{n}$ is the fluctuating electron density, in a toroidal geometry $\tilde{V}_r$ is the fluctuating radial velocity of particles in a plasma cross sec-

[a]Author to whom correspondence should be addressed; electronic mail: x.shi@cqu.edu.au

tion, $\tilde{E}_p$ is the fluctuating poloidal electric field, and B is the toroidal magnetic field. The $P_{\tilde{n}\tilde{E}_p}$ is the cross-power spectrum of $\tilde{n}$ and $\tilde{E}_p$

$$P_{\tilde{n}\tilde{E}_p}(\omega)=F^*_{\tilde{n}}(\omega)F_{\tilde{E}_p}(\omega), \tag{3}$$

where $F_{\tilde{n}(\omega)}$, $F_{\tilde{E}_p}(\omega)$ are the Fourier transforms of $\tilde{n}$ and $\tilde{E}_p$, respectively, and the asterisk denotes the complex conjugate. The Re in the front of the integral in Eq. (2) denotes the real part of the integral.

In order to obtain a ''time-resolved particle flux,'' we replace Eq. (3) with

$$P_{\tilde{n}\tilde{E}_p}(a,b)=\mathrm{CWT}^*_{\tilde{n}}(a,b)\mathrm{CWT}_{\tilde{E}_p}(a,b), \tag{4}$$

where $\mathrm{CWT}^*_{\tilde{n}}(a,b)$ are the complex conjugates of the CWT coefficients of $\tilde{n}$, and $\mathrm{CWT}_{\tilde{E}_p}(a,b)$ are the CWT coefficients of $\tilde{E}_p$. Now Eq. (2) can be rewritten as

$$\langle\tilde{n}\tilde{V}_r\rangle_b=\frac{1}{B}\langle\tilde{n}\tilde{E}_p\rangle_b=\frac{2}{B}\mathrm{Re}\int_0^\infty p_{\tilde{n}\tilde{E}_p}(a,b)da. \tag{5}$$

Equation (5) calculates the total particle flux, which is the sum of the flux contributed from all frequency components, near the time indicated by b. In the CWT spectral technique the flux contributed from the lower frequency components is averaged over longer time windows, while the flux contributed from higher frequency components is averaged over shorter time windows to give a better time resolution to the fast changing particle flux.

III. RESULTS

A. Time-resolved radial particle flux

H-1 is a helical axis stellarator having a major radius of 1.0 m and a mean minor radius of about 0.2 m. The data used in this article were obtained at low magnetic fields (<0.2 T). The plasma was produced and sustained by 50–80 ms pulses of radio frequency power of up to 100 kW at 7 MHz. Electron temperatures in the discharge were low enough (Te =5–30 eV) for probes to be used in the inner regions of the plasma.

In the H-1 heliac, two improved confinement modes were observed, distinguished by fluctuation behavior across the transition to the high confinement mode.[7] In the so-called ''quiescent'' high mode the fluctuation level drops by more than an order of magnitude compared to the low mode. In the ''fluctuating'' high mode fluctuations persist after the transition. Figure 1 shows the ion saturation current and the poloidal electric field in a typical plasma shot, with a transition from the low to the fluctuating high confinement mode approximately 27 ms after the start of the plasma.

In Fig. 1 the ion saturation current I_s and the poloidal electric field E_p are obtained from the measurements of two poloidally separated Langmuir probes positioned at $r/a_p \approx 0.38$, where a_p is the mean radius of the last closed magnetic surface. The Langmuire probe signals were sampled at 200 kHz.

To obtain a time-resolved particle flux, the CWT has been performed on I_s and E_p, respectively. Here we assume

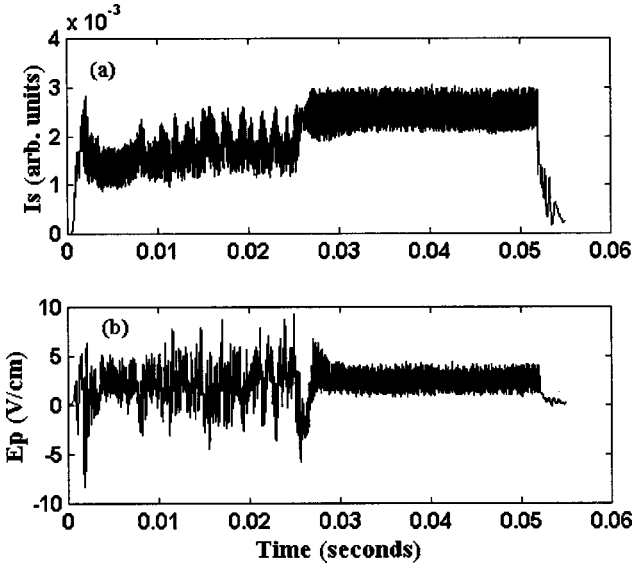

FIG. 1. The ion saturation current (a) and the poloidal electric field (b) measured at the radial position $r/a_p \approx 0.38$, a_p being the mean radius of the last closed magnetic surface. Plasma shot No. 26882.

that $I_s \propto n$. It was found that the main energy of the spectrum of both I_s and E_p is in the frequency range of 4–26 kHz. The CWT magnitude spectra of I_s and E_p in this frequency range are shown in Fig. 2, where the scales are shown to the right on the y axis, with their corresponding frequencies to the left. The magnitudes of the CWT coefficients are shown with gray scales.

In Fig. 2 the dominant frequency component in both I_s and E_p is centered at about 13 kHz in the low confinement mode, and then it drops to about 5 kHz in the high confinement mode. Using Eqs. (4) and (5) in Sec. II the time-resolved radial particle flux is obtained as shown in Fig. 3. The flux contributed from the frequency band centered at about 13 kHz has a time resolution of ~0.16 ms, which is the effective length of the analyzing Morlet wavelet used to analyze that frequency band. While the flux contributed from the frequency band centered at about 5 kHz has a time resolution of ~0.4 ms.

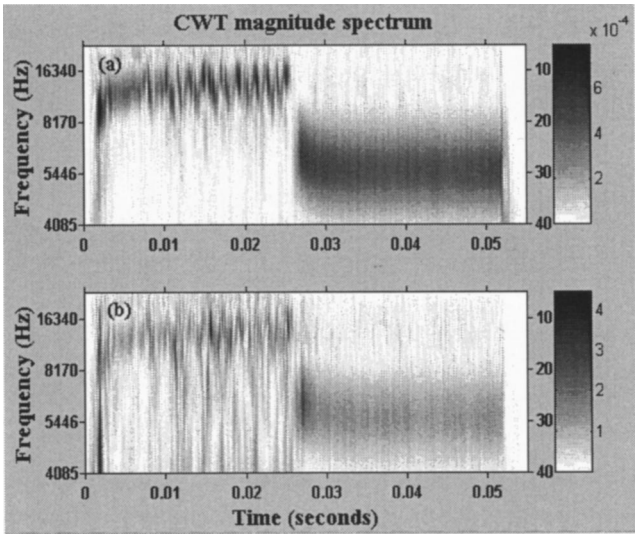

FIG. 2. The CWT magnitude spectrum of I_s (a) and of E_p (b). The scales are shown to the right on the y axis, with their corresponding frequencies to the left; the magnitudes of the coefficients are shown in gray scales.

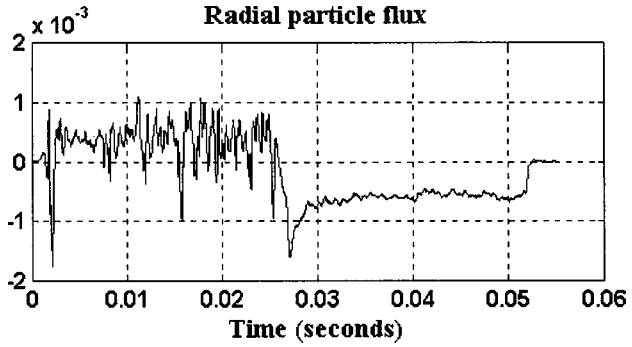

FIG. 3. Time-resolved radial particle flux in arbitrary units.

The flux shown in Fig. 3 oscillates with its average directed outwards in the low confinement mode. A clear flux reversal occurs at about 27 ms into the discharge. In the fluctuating high confinement mode, the flux is directed steadily inwards. The modification in particle transport during and after the low to the fluctuating high confinement mode transition observed in H-1 is mainly due to the change of the relative phase between the I_s and E_p.[8]

B. Dependence of the fluctuation frequency on the radial electric field

It has been shown in Ref. 9 that the fluctuations in the low confinement mode in H-1 propagate in the lab frame with the **E×B** drift velocity. Here we attempt to find a correlation between the time-resolved fluctuation frequency obtained using CWT and the average radial electric field in H-1. The results are shown in Fig. 4.

The data in Fig. 4 is from a plasma shot, which exhibits a transition from the low to the quiescent high confinement mode at approximately 50 ms into the discharge. In Fig. 4(b), the average radial electric field E_r is derived from the plasma potentials measured by two triple probes:[10] one fixed at $r/a_p \approx 0.33$ and another at $r/a_p \approx 1$. The dominant frequency component as a function of time shown in Fig. 4(c) was obtained from the CWT spectrum of the ion saturation current signal shown in Fig. 4(a).

It is shown in Fig. 4 that the frequency of the dominant fluctuation component closely follows changes in the electric field during the time interval when the plasma is in the low confinement mode (up to 50 ms). This result supports the view that the frequency observed in the lab frame is due to the **E×B** Doppler shift. The idea of estimating the time-resolved plasma rotation velocity from the evolution in the fluctuation frequency has also been used in the recent experiments on the DIII-D tokamak.[11]

IV. SUMMARY

It has been shown that the time-resolved turbulence-driven radial particle flux in plasma can be estimated using the CWT spectral technique. This technique might be particularly useful when studying the behavior of the turbulent transport in nonstationary plasma conditions, like, for example, dithering cycles. The results presented in this article

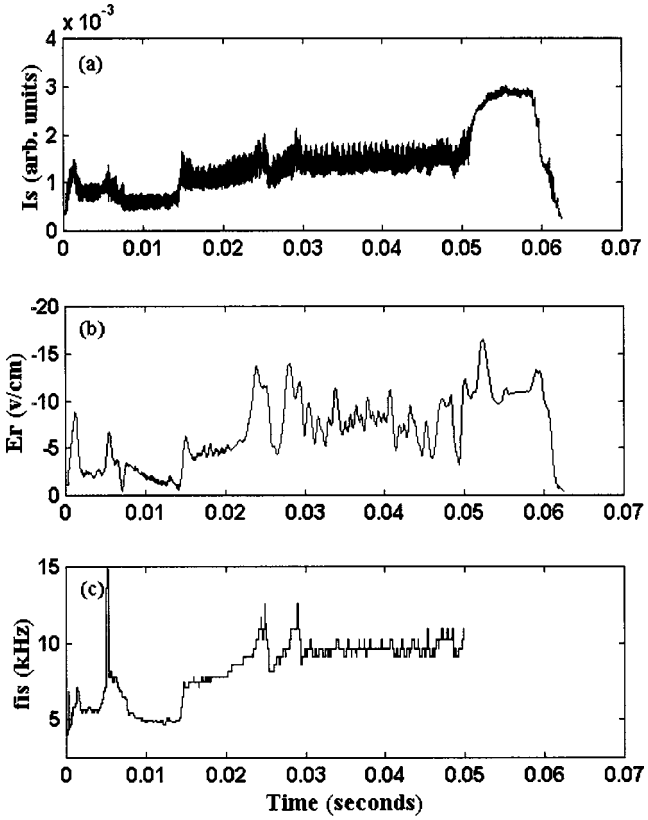

FIG. 4. (a) The ion saturation current measured at the radial position $r/a_p \approx 0.38$, a_p being the mean radius of the last closed magnetic surface. (b) The average radial electric field. (c) The dominant frequency component in the ion saturation current. Plasma shot No. 27469.

confirm that the radial flux reverses during the transition from the low to the fluctuating high confinement mode in the H-1 heliac as discussed in Refs. 7–9.

A strong correlation between the fluctuation frequency and the radial electric field has also been visualized using the CWT. The application of wavelet analysis to the temporal evolution of the fluctuation frequency in a situation when the fluctuation phase velocity in the lab frame is dominated by the $E \times B$ drift can (with certain caution) be used as a diagnostic tool to estimate the time-resolved radial electric field.

ACKNOWLEDGMENT

The authors thank the Australian Institute of Nuclear Science and Engineering (AINSE) for sponsoring this collaboration.

[1] V. Dose, G. Venus, and H. Zohm, Phys. Plasmas **4**, 323 (1997).
[2] B. Ph. van Milligen, E. Sanchez, T. Estrada, C. Hidalgo, B. Branas, B. Carreras, and L. Garcia, Phys. Plasmas **2**, 3017 (1995).
[3] M. V. A. P. Heller, Z. A. Brasilio, I. L. Caldas, and R. M. Castro, Czech. J. Phys. **48**, 125 (1998), Suppl. S3.
[4] E. J. Powers, Nucl. Fusion **14**, 749 (1974).
[5] A. V. Oppenheim and R. W. Schafer, *Discrete-Time Signal Processing* (Prentice-Hall, Englewoad Cliffs, NJ, 1989).
[6] I. Daubechies, *Ten Lectures on Wavelets* (SIAM, Philadelphia, PA, 1992).
[7] M. G. Shats, Plasma Phys. Controlled Fusion **41**, 1357 (1999).
[8] M. G. Shats *et al.*, Phys. Rev. Lett. **84**, 6042 (2000).
[9] M. G. Shats and D. L. Rudakov, Phys. Rev. Lett. **79**, 2690 (1997).
[10] D. L. Rudakov, M. G. Shats, R. W. Boswell, C. Charles, and J. Howard, Rev. Sci. Instrum. **70**, 476 (1999).
[11] T. L. Rhodes, F. L. Hinton, K. H. Burrell, R. J. Groebner, W. A. Peebles, C. L. Rettig, and M. R. Wade, Nucl. Fusion **39**, 1051 (1999).